Duration and Ice Thickness of a Late Holocene Outlet Glacier Advance near Narsarsuaq, South Greenland

Peter J.K. Puleo[1] and Yarrow Axford[1]

[1]Department of Earth and Planetary Sciences, Northwestern University, Evanston, 60201, USA

5 *Correspondence to*: Peter J.K. Puleo (peterpuleo2024@u.northwestern.edu)

Abstract. Greenland Ice Sheet (GrIS) outlet glaciers are currently losing mass, leading to sea level rise. Reconstructions of past outlet glacier behavior through the Holocene help us better understand how they respond to climate change. Kiattuut Sermiat, a south Greenland outlet glacier near Narsarsuaq, is known to have experienced an unusually large Late Holocene advance that culminated at ~1600 cal yr BP and exceeded the glacier's Little Ice Age extent. We report sedimentary records

10 from two lakes at slightly different elevations in an upland valley adjacent to Kiattuut Sermiat. These reveal when the outlet glacier's surface elevation was higher than during the Little Ice Age and constrain the associated outlet glacier surface elevation. We use bulk sediment geochemistry, magnetic susceptibility, color, texture, and the presence of aquatic plant macrofossils to distinguish between till, glaciolacustrine sediments, and organic lake sediments. Our ^{14}C results above basal till recording regional deglaciation skew slightly old due to a reservoir effect but are generally consistent with regional

15 deglaciation occurring ~11,000 cal yr BP. Neoglacial advance of Kiattuut Sermiat is recorded by deposition of glaciolacustrine sediments in the lower-elevation lake, which we infer was subsumed by an ice-dammed lake that formed along the glacier's margin just after ~3900 cal yr BP. This timing is consistent with several other glacial records in Greenland showing Neoglacial cooling driving advance between ~4500-3000 cal yr BP. Given that glaciolacustrine sediments were deposited only in the lower-elevation lake, combined with glacial geomorphological evidence in the valley containing these lakes, we estimate the

20 former ice margin's elevation to have been ~670 m a.s.l., compared with ~420 m a.s.l. today. The ice-dammed lake persisted until the glacier surface fell below this elevation at ~1600 cal yr BP. The retreat timing contrasts with overall evidence for cooling and glacier advance in the region at that time, so we infer that Kiattuut Sermiat's retreat may have resulted from reduced snowfall amounts and/or local glaciological complexity. High sensitivity to precipitation changes could also explain the relatively limited Little Ice Age advance of Kiattuut Sermiat compared with the earlier Neoglacial advance.

1 Introduction

The Greenland Ice Sheet (GrIS) today is losing mass and is one of the largest contributors to global sea level rise in response to anthropogenic warming (Dowdeswell, 2006; Goelzer et al., 2020; Greve and Chambers, 2022). The amount of sea level rise contributed by the GrIS is highly dependent on future emission scenarios (Goelzer et al., 2020; Greve and Chambers, 2022).

30 Much of this mass is lost through outlet glaciers, making understanding how and why the dynamics of outlet glaciers have changed over time vital for improving estimates of future GrIS contributions to sea level rise (Goelzer et al., 2020).

The ice sheet's history during the warming and cooling phases of the Holocene provides insights into how outlet glaciers and overall ice sheet mass balance respond to climate change. Here, we focus on south Greenland, where past work has constrained aspects of the Holocene ice sheet and climate history. Increases in Northern Hemisphere summer insolation (Berger and Loutre,

35 1999) and greenhouse gases (Monnin et al., 2001) drove abrupt overall warming in Greenland following the Last Glacial Maximum (Buizert et al., 2018). South Greenland is also particularly sensitive to changing Atlantic meridional overturning circulation conditions, like those that occurred in the Younger Dryas (~12,900-11,700 cal yr BP) and drove abrupt temperature shifts (Puleo et al., 2022). Abrupt deglacial warming led to rapid regional deglaciation around south Greenland, which occurred by ~12,300 cal yr BP near Qaqortoq (Levy et al., 2020) and ~11,100-10,500 cal yr BP near Narsarsuaq (Larsen et al., 2011;

40 Carlson et al., 2014; Nelson et al., 2014). In the Early to Middle Holocene, elevated Northern Hemisphere summer insolation (Berger and Loutre, 1999) drove further warming during the Holocene Thermal Maximum (~9000-5000 cal yr BP; Axford et al. 2021). In south Greenland, the southernmost GrIS ice margin was behind its present extent for some time between ~7000 to 3000 cal yr BP in response to warmth that probably peaked in this region between ~7300 and 5500 cal yr BP (Kaplan et al., 2002; Larsen et al., 2011; Larsen et al., 2015; Larocca et al. 2020a). Subsequent Neoglacial cooling in the Middle and especially

45 late Holocene drove glacier growth around much of Greenland, including in the south (Larsen et al., 2011; Larocca et al., 2020a). Many glaciers reached their maximum Late Holocene positions during the Little Ice Age (Kelly and Lowell, 2009; Kjær et al., 2022), but exceptions hint at complex patterns of Late Holocene glacier change.

One notable exception is the Narsarsuaq advance in south Greenland. The Narsarsuaq advance of Kiattuut Sermiat (Kiagtût Sermiat; Bjørk et al., 2015), one of the southernmost GrIS outlet glaciers, had a culmination timing of outermost moraines at

50 ~1500 cal yr BP based on [10]Be and lake sediment ^{14}C dating (Weidick, 1963; Bennike and Sparrenbom, 2007; Winsor et al., 2014; Nelson et al., 2014). Retreat of Kiattuut Sermiat at ~1500 cal yr BP is not consistent with nearby temperature reconstructions that indicate cooling at this time (Wooller et al., 2004; Fréchette and de Vernal, 2009; Lasher et al., 2019). The onset timing of this advance is unconstrained, and its magnitude greatly exceeded the extent of the Kiattuut Sermiat Little Ice Age advance (Winsor et al., 2014).

55 To determine the duration and timing of the Narsarsuaq advance, we collected sediment cores from two lakes situated within an upland valley that is tributary to the valley of Kiattuut Sermiat. Geomorphological and sedimentological evidence suggest this valley was ice-dammed by the expanded outlet glacier during the Narsarsuaq advance. Sediment records from the two threshold lakes, which sit at slightly different elevations, also allow us to precisely constrain the maximum elevation of the outlet glacier surface (ice dam) during the advance.

60

2 Study Area

Kiattuut Sermiat, an outlet glacier of the GrIS, is located ~10 km northeast of Narsarsuaq and is adjacent to the Mellemlandet plateau (Fig. 1B). Kiattuut Sermiat flows to the southwest and feeds the Narsarsuaq river that runs into the Tunugdliarfik fjord. Informally named lakes LMEL (Lower Mellemlandet; 61.2423°N, 45.2217°W) and UMEL (Upper Mellemlandet; 61.2373°N,

65 45.2282°W) are located in an east-west trending valley on Mellemlandet, an ice-free, high-elevation, northeast-southwest

trending bedrock ridge that divides Kiattuut Sermiat from the adjacent outlet glacier Qooqqup Sermia (Qôrqup Sermia; Bjørk et al., 2015; Figs. 1B, C). Satellite images and digital elevation models (DEMs; Porter et al., 2018) show landscape features west of the lakes, including paleoshorelines, lateral moraines, and probably subaqueous moraines, that record a time when Kiattuut Sermiat advanced into the east-west valley that contains the lakes (Figs. 1D and E). The corresponding paleoglacier's advanced position would have dammed the valley, and thus the lake system's outlet stream, and created a proglacial lake. Depending upon its depth and extent, this proglacial lake could have subsumed LMEL and possibly UMEL.
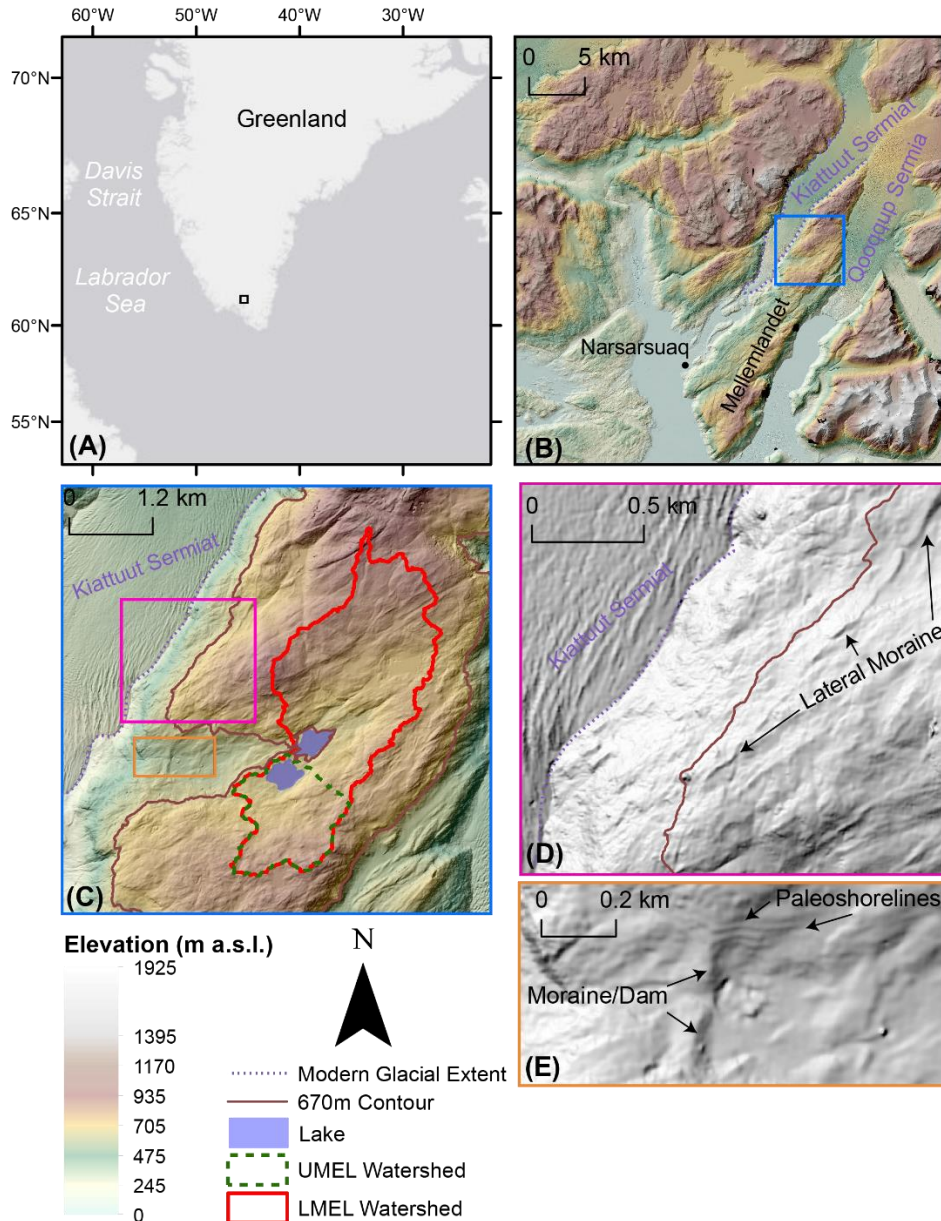
Figure 1 (A) Map of south Greenland (ESRI). Black square shows the extent of panel B. (B) Shaded relief digital elevation model (DEM) of the region around Narsarsuaq (Porter et al., 2018). Blue square shows the extent of panel C. (C) DEM with LMEL and UMEL and their watersheds (in solid red and dashed green outlines, respectively). The brown line indicates the 670 m a.s.l. contour. Pink square shows the extent of panel D. Orange rectangle shows the extent of panel E. (D) DEM showing a lateral moraine of Kiattuut Sermiat, and 670 m a.s.l. contour in brown. (E) DEM showing an associated moraine and paleoshoreline features.

LMEL is 0.12 km^2 and has an elevation of ~670 meters above sea level (m a.s.l.). Its maximum depth is ~28 m and its watershed area is 7.0 km^2 (Fig. 1C). UMEL is 0.13 km^2 and has an elevation of ~675 m a.s.l. Its maximum depth is ~26 m and its watershed area is 1.9 km^2 (Fig. 1C). Both lakes have no glaciers in their watershed at present and are ~2.5 km east of (and ~250 m above the modern-day elevation of) Kiattuut Sermiat. The vegetation cover in the watershed was estimated at ~70% in July 2019 and includes *Chamaenerion latifolium*, *Empetrum nigrum*, and *Betula nana*. The bedrock of the Mellemlandet ridge is largely granite and granodiorite with some metasedimentary gneiss (~1800 Ma; Julianehåb igneous complex; Steenfelt et al., 2016) along with syenite, gabbro, and carbonatite dykes (~1300-1,140 Ma; Gardar Province; Upton et al., 2003), the last of which may contribute ancient inorganic carbon to LMEL and UMEL.

The closest meteorological station is located in Narsarsuaq (~10 km SW of LMEL and UMEL). Mean annual air temperature in Narsarsuaq from 1981-2010 was 1.1°C (Cappelan, 2019). Mean monthly temperatures range from -7.3°C (February) to 10.8°C (July). The mean annual precipitation amount from 1981-2010 was 650.7 mm with the mean monthly precipitation amounts slightly weighted to the summer and fall. Mean temperatures at LMEL and UMEL are likely lower due to the higher elevation of the sites compared to the Narsarsuaq station (30 m a.s.l.).

3 Methods

3.1 Sediment Core Collecting and Sediment Characterization

In July 2019, we collected several sediment cores from LMEL and UMEL (Table 1). From LMEL, we focus on 19-LMEL-N2, 19-LMEL-U11, and 19-LMEL-U5 (recovered from 12.3, 8.0, 18.9 m water depth, respectively). These cores were selected due to their relatively long length and representation of varied water depths and locations within the lake. From UMEL, two cores were collected (19-UMEL-U2 at 12 m water depth and 19-UMEL-U1 at 24.5 m water depth). 19-LMEL-N2 was collected with a Nesje percussion piston coring device (Nesje, 1992) while the other cores were collected with an Aquatic Research Instruments "Universal" open-valve coring device designed to capture an intact sediment-water interface.

The sediment cores were split using a GeoTek core splitter and stored at 4°C. Magnetic susceptibility (MS), visible color reflectance, and elemental abundance of freshly split cores were measured every 2 mm using a Geotek MSCL-S equipped with a Bartington MS2E point sensor, a Konica Minolta CM-700d spectrophotometer, and an Olympus DELTA Professional X-Ray Fluorescence (XRF) spectrometer. Cores were topped with 4 µm Ultralene film prior to scanning. XRF measurements had a 30 second dwell time.

Table 1 Core sampling location information. For the Core Name column: U=Universal (check valve) core and N=Nesje (piston) core.

Lake	Core Name	Latitude (°N)	Longitude (°W)	Water Depth (m)	Core Length (m)
UMEL	U1	61.23745	45.22714	24.5	0.535
UMEL	U2	61.23750	45.22868	12	0.910
LMEL	U5	61.24208	45.21881	18.9	1.690
LMEL	U11	61.24088	45.22044	8.0	1.485
LMEL	N2	61.24239	45.22174	12.3	2.615

Many sedimentological properties have been used to infer glacial changes based on lake sediments. Glaciers typically drive increased delivery of fine-grained, minerogenic material to lakes via bedrock erosion and glacial meltwater transport. Thus, when glaciers are present in a watershed, lake waters are often turbid and aquatic primary production is low. The resulting lacustrine sediments have a relatively small amount of organic material and consist largely of minerogenic silt/clay (occasionally with some larger, unsorted grains), with these properties often clearly reflected in sediment color (Karlen and Matthews, 1992; Balascio et al., 2015; Adamson et al., 2022; Larocca and Axford, 2022). Additionally, glacier-influenced lacustrine sediments are characterized by relatively large concentrations of elements found in local bedrock (e.g., Ti) and often high MS values from abundance of iron-bearing mineral grains and low abundance of biogenic materials (Karlen and Matthews, 1992; Larsen et al., 2011; Larocca et al., 2020a). Following the precedent of numerous studies in southwest/south Greenland (e.g., Larsen et al., 2011, 2015; Schweinsberg et al., 2017, 2018; Larocca et al., 2020a, 2020b), we infer glacier influence on our study lakes from Ti abundance, MS, and qualitative assessments of grain size and organic content (the latter based on sediment color, where gray indicates lower organic content and brown indicates higher organic content).

3.2 Sediment Core Chronology

Terrestrial plant remains, aquatic moss remains, and bulk sediments were sampled from 19-LMEL-N2 (n=7), 19-LMEL-U11 (n=12), 19-LMEL-U5 (n=2), and 19-UMEL-U2 (n=5) and submitted to the Woods Hole Oceanographic Institution National Ocean Sciences Accelerator Mass Spectrometry (WHOI NOSAMS) for Accelerator Mass Spectrometry ^{14}C analysis (Table 2). Most radiocarbon samples were collected immediately above or below clear sedimentological transitions, and we sampled terrestrial plant remains where possible to avoid potential reservoir effects. Bulk sediments were sampled as a last resort where no adequate plant macrofossils were uncovered. Bulk sediment ^{14}C samples were paired with plant macrofossils at several

depths to evaluate the efficacy of ^{14}C in bulk sediments. Radiocarbon ages were calibrated using CALIB version 8.2 (Stuiver et al., 2022) and the IntCal20 calibration curve (Reimer et al., 2020).

135

Table 2 Radiocarbon samples from LMEL and UMEL sediment cores with ^{14}C and calibrated ages.

Core	Sample ID	Depth in Sediment (cm)	Material	Fraction Modern	^{14}C Age (^{14}C yr BP)	^{14}C Age Error (2σ)	Median Cal. Age (cal yr BP)	Min. Cal. Age (cal yr BP, 2σ)	Max. Cal Age (cal yr BP, 2σ)
19 LMEL N2	176106	7.5	Aquatic Moss	0.7952	1840	20	1740	1710	1820
19 LMEL N2	176107	8.5	Aquatic Moss	0.7944	1850	20	1760	1710	1820
19 LMEL N2	176110	210.5	Sediment	0.5705	4510	25	5150	5050	5300
19 LMEL N2	176111	217.5	Sediment	0.3029	9590	60	10,940	10,730	11,170
19 LMEL N2	176108	217.5	Aquatic Moss	0.2912	9910	45	11,310	11,220	11,600
19 LMEL N2	176112	220	Sediment	0.2838	10,100	50	11,670	11,400	11,880
19 LMEL N2	176109	220	Aquatic Moss	0.2767	10,300	45	12,070	11,840	12,460
19 LMEL U11	176116	10.5	Aquatic Moss	0.7795	2000	20	1940	1880	1990
19 LMEL U11	176115	20.5	Aquatic Moss	0.7298	2530	20	2620	2500	2740
19 LMEL U11	176767	29.25	Terrestrial Plant	0.8392	1410	25	1320	1290	1350
19 LMEL U11	176114	31.5	Terrestrial Plant / Aquatic Moss	0.8092	1700	15	1580	1540	1670
19 LMEL U11	176113	32.5	Aquatic Moss	0.7618	2190	25	2240	2120	2310
19 LMEL U11	176117	32.5	Sediment	0.7293	2540	20	2630	2520	2740
19 LMEL U11	176121	132.5	Sediment	0.6046	4040	25	4480	4420	4570
19 LMEL U11	176122	133.5	Sediment	0.5974	4140	20	4690	4580	4820
19 LMEL U11	176118	133.5	Terrestrial Plant	0.6410	3570	35	3870	3720	3980
19 LMEL U11	176119	140	Terrestrial Plant	0.4688	6090	35	6950	6800	7160
19 LMEL U11	176123	147	Sediment	0.4217	6940	35	7760	7680	7910
19 LMEL U11	176120	147	Terrestrial Plant	0.4874	5770	30	6570	6490	6660

19 LMEL U5	176130	22.5	Sediment	0.7787	2010	20	1950	1890	2000
19 LMEL U5	176129	23.5	Sediment	0.7590	2220	20	2230	2150	2320
19 UMEL U2	176128	18.5	Aquatic Moss	0.7694	2110	20	2070	2000	2140
19 UMEL U2	176127	36	Terrestrial Plant	0.7003	2860	25	2980	2880	3070
19 UMEL U2	176126	58	Terrestrial Plant	0.4079	7200	40	8000	7940	8170
19 UMEL U2	176125	73.5	Aquatic Moss	0.2939	9840	50	11,250	11,180	11,390
19 UMEL U2	176124	78	Aquatic Moss	0.2813	10,200	50	11,870	11,640	12,050

3.3 Watershed Development and Elevation History

140 We modeled watershed areas for LMEL and UMEL using the ESRI ARCMap Hydrology toolset and the 2 m resolution ArcticDEM (Porter et al., 2018). Modern topography, lake elevations, and watershed boundaries were used to estimate the past elevation of the Kiattuut Sermiat ice dam during periods when lake sediments reveal LMEL was subsumed by a proglacial lake.

4 Results

4.1 Sediment Properties

19-LMEL-N2 is 261.5 cm long and its sediments comprise two primary units (and three subunits of Unit 1) based on changes in color, grain size, presence of organic matter, MS, and sediment chemistry (Fig. 2). Unit 2 (261.5-224 cm), the lowermost unit, is a gray, poorly sorted diamicton with pebbles and granules in a matrix of silt/clay and has no visible organic materials.

150 Much of the unit could not be scanned due to unevenness of the split core surface around its large grains; however, the uppermost part of the unit was scannable and has relatively high MS and Ti values. Unit 2 does not have well preserved internal stratigraphy. The overlying Unit 1 comprises horizontally bedded and relatively well-sorted sediments. Unit 1c (224-210 cm) consists of horizontally bedded, brown, fine-grained sediments with some aquatic moss remains, and low values of MS and Ti. Unit 1b (210-10 cm) is laminated to coarsely layered, light to dark gray silt/clay without visible organics or macrofossils.

155 It has relatively high values of MS throughout with some variability in Ti. The uppermost Unit, 1a (10-0 cm), is brown with some black laminations and contains a large amount of aquatic moss remains. The Unit 1a sediments are characterized by low MS and low Ti concentrations.
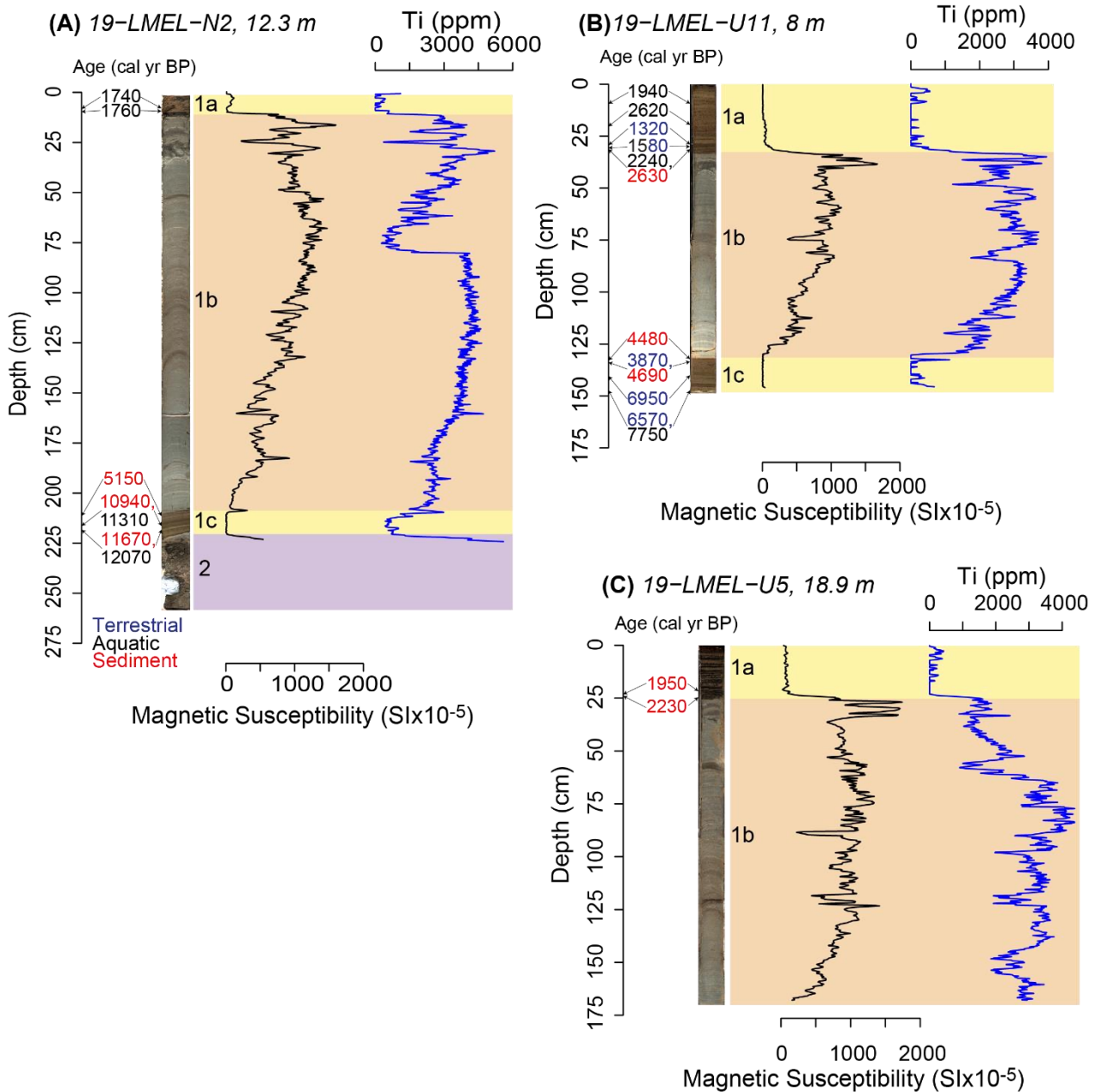
Figure 2 (A) Core 19-LMEL-N2. (B) Core 19-LMEL-U11. (C) Core 19-LMEL-U5. Sediment core stratigraphy, sedimentary units, magnetic susceptibility (MS), and titanium abundance (Ti) for three cores from LMEL Lake. Numbers and arrows to the right of the depth axis indicate calibrated ages inferred from ^{14}C ages (terrestrial plant ages in blue, aquatic plant ages in black, and bulk sediment ages in red). Units are shown as colored and labeled rectangles to the right of each core image. Water depth is listed after the core name.

165 19-LMEL-U11 is 148.5 cm long and contains the three uppermost units contained within 19-LMEL-N2 (Fig. 2). Unit 1c (148.5-132 cm) is brown, laminated, organic, fine-grained sediment that contains terrestrial plant and aquatic moss remains, and has relatively low MS and Ti values. Unit 1b (132-34 cm) is gray, coarsely bedded to finely laminated silt/clay, contains no visible plant macrofossils, and has high MS and Ti concentrations. Unit 1a (34-0 cm) is very similar to Unit 1c, as it is brown, contains terrestrial and aquatic plant remains, and returns to low MS and Ti values. This core has a well-preserved

170 sediment-water interface.

19-LMEL-U5 is 169 cm long and has two units similar to the two uppermost units of 19-LMEL-N2 and 19-LMEL-U11 (Fig. 2). Unit 1b (169-25 cm) is gray, composed of silt/clay, and contains no obvious plant macrofossils. It has relatively high values of MS and Ti and the color also suggests low organic content. Unit 1a (0-25 cm) is brown, organic, fine-grained sediment with many black laminations and has MS and Ti values close to zero. This unit contains few plant macrofossils, unlike Unit 1a in

175 19-LMEL-N2 and 19-LMEL-U11. The sediment-water interface is well preserved.

From the higher-elevation lake, core 19-UMEL-U2 is 91 cm long and contains two units (Fig. 3). Unit 2 (91-79 cm) of this core is similar to Unit 2 of 19-LMEL-N2, a gray diamicton with pebbles and granules in a matrix of silt/clay, with no visible organic materials or clear internal stratigraphy. The diamicton has relatively high values of MS and Ti. Unit 1 (79-0 cm) has similar characteristics to Units 1a and 1c in the LMEL cores. It is made up of brown, organic, laminated, fine-grained sediment containing abundant aquatic moss remains with relatively low MS and low Ti values. The sediment-water interface was slightly

180 disturbed during coring.
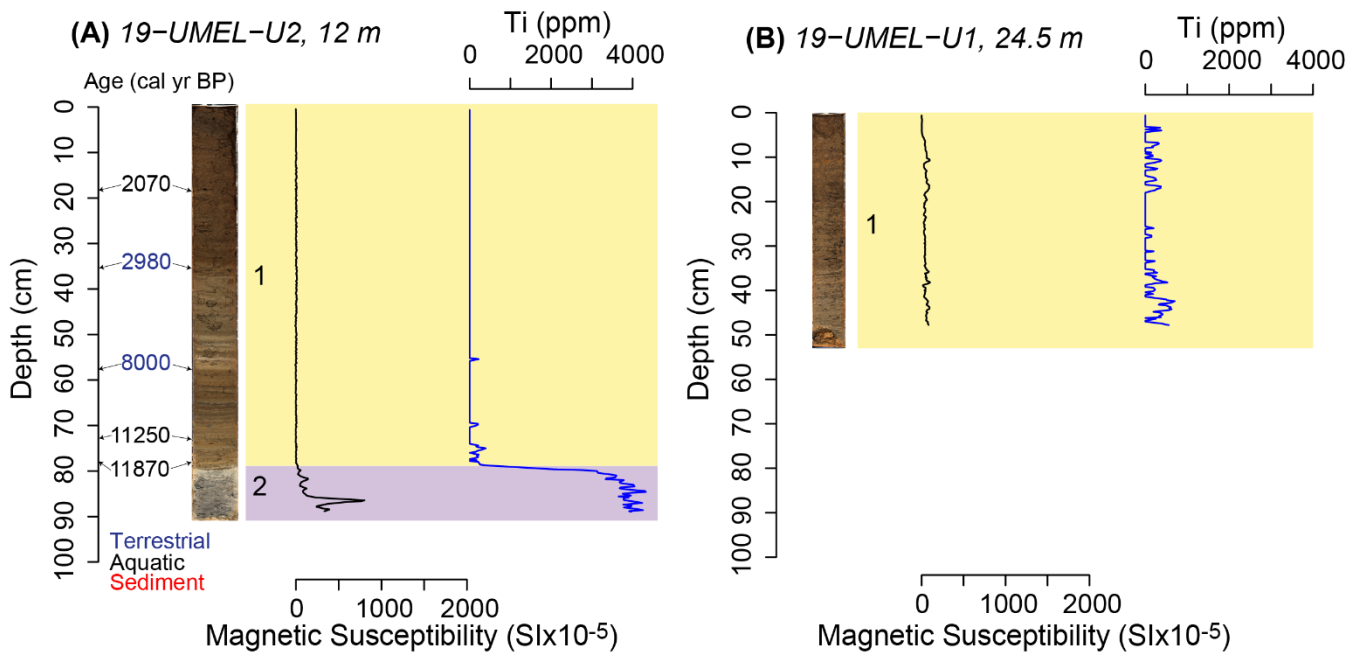
Figure 3 (A) Core 19-UMEL-U2. (B) Core 19-UMEL-U1. Sediment core stratigraphy, units, MS, and Ti for two cores from UMEL Lake. Numbers and arrows to the right of the depth axis indicate calibrated ages inferred from ^{14}C ages (terrestrial plant ages in blue, aquatic plant ages in black, and bulk sediment ages in red). Colored and labeled rectangles to the right of the core image correspond to units. Water depth is listed after the core name.

19-UMEL-U1 is 53.5 cm long and contains only the lake's uppermost sedimentary unit (Fig. 3). Unit 1 is a brown, organic-rich fine-grained laminated sediment very similar to Unit 1 of 19-UMEL-U2 and Units 1a/1c of the LMEL cores.

4.2 Sediment Core Chronology

Radiocarbon sampling focused on constraining the ages of the sedimentary unit transitions described above. Due to the infrequent occurrence of terrestrial plant macrofossils in the lake sediments, combined with the mapped occurrence of potentially carbon-bearing bedrock and/or glacial drift in the region, we dated multiple organic material types and aimed to assess reservoir effects on ^{14}C in aquatic moss and bulk organic materials. In all cases and across a range of time periods, terrestrial plant samples yielded younger apparent ages than aquatic moss or bulk sediment samples from the same depth (Fig. 4; Table 2), leading us to suspect a lacustrine reservoir effect. We argue that this more specifically reflects a hardwater effect resulting from the regional presence of ancient carbon-bearing rocks, including carbonate-rich carbonatite (Upton et al. 2003). Inputs of ancient dissolved inorganic carbon to the lake via ice sheet meltwater could also cause ^{14}C reservoir effects (Björck and Wohlfarth, 2001), as could long-term perennial ice cover, but both are unlikely here. Glacial meltwater inputs would only have affected radiocarbon samples taken from times when glacier meltwater flowed into LMEL or UMEL. This would be the times of Narsarsuaq Advance (for LMEL) and the earliest deglacial period (for both lakes), neither of which were sampled to determine radiocarbon ages. As for ice cover limiting atmospheric CO2 exchange, modern LMEL and UMEL experience many ice-free months in summer and these small, relatively shallow lakes are well mixed then by the wind. Thus, we infer a reservoir effect attributable to the regional presence of carbonatites and other carbon-bearing rocks. Because of this, ages on aquatic mosses and bulk sediments are treated here as loose maximum estimates of depositional age, whereas ages on terrestrial plants provide tighter constraints on depositional age.
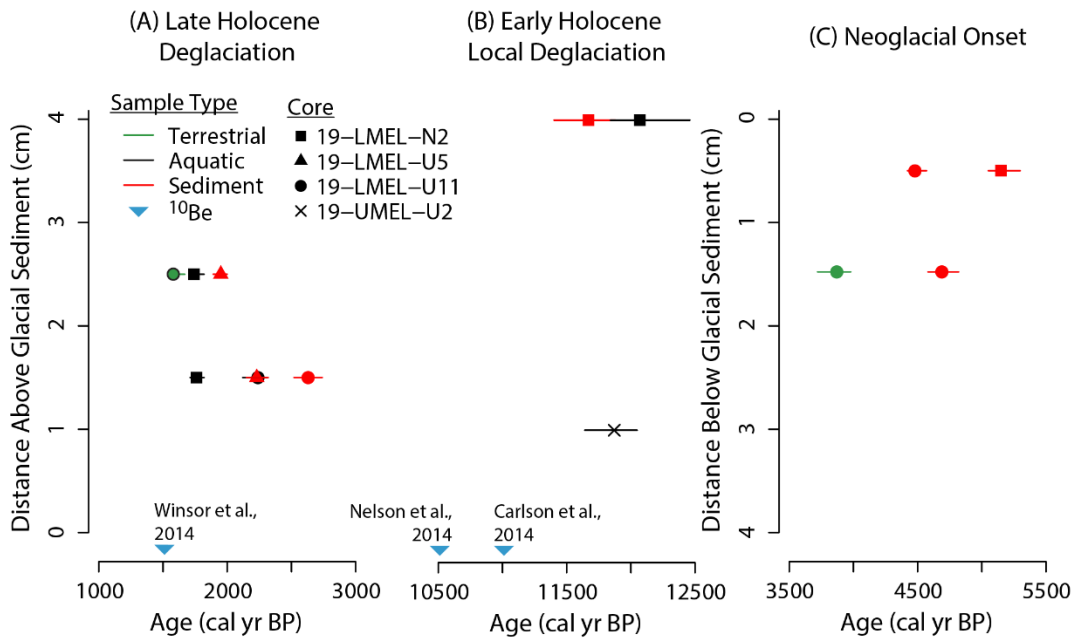
Figure 4 Key radiocarbon ages near sedimentological transitions in four sediment cores from LMEL and UMEL. Note that ages from aquatic mosses (black) and bulk sediments (red) are presumed too old but provide loose maximum estimates of the timing of organic matter deposition. (A) Ages from above inorganic, glaciolacustrine sediments that constrain the timing of Late Holocene outlet glacier retreat (minimum limiting ages). (B) Ages from above glacial diamicton that constrain local deglaciation in the Early Holocene (minimum limiting ages, but with reservoir effects from carbonate-bearing regional bedrock). (C) Ages from below inorganic, glaciolacustrine sediments that constrain the timing of Middle to Late Holocene outlet glacier advance (maximum limiting ages).

The transition from diamicton to laminated sediments (from Unit 2 to Unit 1c in 19-LMEL-N2 and from Unit 2 to Unit 1 in 19-UMEL-U2) is constrained by ages of 12,070, 11,670, and 11,870 cal yr BP on two aquatic moss samples and one sediment sample from 1-4 cm above the transition (Fig. 4; Table 2). Stratigraphically, these are minimum limiting ages on the onset of laminated, organic sediment deposition (i.e., the inferred onset of lacustrine deposition), but because of the suspected ^{14}C reservoir effect these ages are likely at least several hundred years older than their actual timing of deposition so we do not treat them as such. Rather, these ages provide very loose estimates of timing. The transition from organic Unit 1c to inorganic Unit 1b in 19-LMEL-N2 and 19-LMEL-U11 likely occurred sometime after ~5200-3900 cal yr BP based on ^{14}C ages of one terrestrial plant sample and three sediment samples 1.5-0.5 cm below the transition (Fig. 4; Table 2). Finally, the most recent transition from inorganic Unit 1b to organic Unit 1a in all of the LMEL cores occurred sometime before ~1600 cal yr BP based

on the ^{14}C age of one mixed terrestrial/aquatic plant sample, three aquatic moss samples, and three sediment samples from 2.5-1.5 cm above the transition (Fig. 4; Table 2).

5 Discussion

5.1 Interpretation of Sediments

We interpret the diamicton, Unit 2 in LMEL and UMEL (Figs. 2 and 3), as subglacial till deposited just prior to local deglaciation by the GrIS as the ice sheet retreated rapidly in the late glacial/Early Holocene from its Last Glacial Maximum position beyond Greenland's modern-day coastline. Similar units are reported from other lakes in Greenland (e.g., Larsen et al., 2011). Unit 2 is only present in the longest core from each lake. Above the diamicton, both lakes contain fine-grained, laminated to bedded sediments (Unit 1c in LMEL and Unit 1 in UMEL) that we interpret as lacustrine. At the higher-elevation lake UMEL, Unit 1 is composed entirely of laminated, tan/brown organic-rich lake sediments with low MS and Ti values and abundant aquatic mosses (Fig. 3). We infer that UMEL sedimentation has not been influenced by glacier fluctuations since regional deglaciation. This system has maintained biologically productive, clear waters that support photosynthesis by aquatic mosses throughout the Holocene since regional deglaciation.

In contrast, Unit 1 of the lower-elevation lake LMEL contains both organic and inorganic lacustrine units (Fig. 2). Unit 1c is finely laminated, tan/brown organic sediments with relatively low Ti and MS values. This unit records the establishment of a biologically productive lake with very little influx of mineral material following local deglaciation. Unit 1c is not recorded by 19-LMEL-U5 because it is the shortest core. Following the precedent of many past studies (Karlen and Matthews, 1992; Balascio et al., 2015; Adamson et al., 2022; Larocca and Axford, 2022), Unit 1b of 19-LMEL-N2, 19-LMEL-U11, and 19-LMEL-U5 is interpreted as glaciolacustrine due to its relatively high MS and Ti values, gray color, silt/clay grain size, horizontal bedding, and absence of visible organic materials. Given the lake's setting, as described in the Study Area section above, glaciolacustrine deposition in LMEL is best explained by a Late Holocene readvance of Kiattuut Sermiat. The outlet glacier thickened enough to enter the east-west valley that contains LMEL (Fig. 1C) and dammed the lake system's outlet stream to create a large ice-marginal lake that subsumed LMEL. Above the glaciolacustrine sediments, Unit 1a of 19-LMEL-N2, 19-LMEL-U11, and 19-LMEL-U5 contains laminated, tan/brown, organic sediments with abundant aquatic mosses. This is interpreted as recording the retreat of Kiattuut Sermiat from its high lateral moraine in the Late Holocene. This allowed the temporary, Late Holocene proglacial lake to drain to an elevation below that of LMEL, which removed the glacial sediment source and enhanced biological production in LMEL. Differences in unit thickness between the three LMEL cores are attributable to different sedimentation rates at the core site locations, which have different water depths.

5.2 Local Greenland Ice Sheet Deglaciation

The transition from diamicton to organic lake sediments at LMEL and UMEL records local deglaciation by the GrIS. Minimum-limiting ^{14}C ages just above these transitions (1-4 cm above; N=3; Fig. 4; Table 2) suggest they occurred before ~11,700 cal yr BP. In general, this is consistent with existing deglacial estimates from sites closer to the coast, where

deglaciation happened earlier: ~14,800 cal yr BP at Nanortalik (Levy et al., 2020), ~13,600 cal yr BP from Lake N14 at the southern tip of Greenland (Björck et al., 2002; Puleo et al., 2022), ~13,400 cal yr BP at Pamiagdluk (Levy et al., 2020), and ~12,300 cal yr BP at Qaqortoq (Levy et al., 2020). However, our local deglaciation ages are earlier than suggested by [10]Be dates on boulders and bedrock near Kiattuut Sermiat and closest to our sites (~6.5 km southeast; Carlson et al., 2014; Nelson
265 et al., 2014). Carlson et al. (2014) suggest deglaciation between 11,100-10,600 cal yr BP and Nelson et al., 2014 suggest deglaciation at ~10,500 cal yr BP. This apparent discrepancy can be explained by the lake water reservoir effect we have identified on aquatic materials dated at LMEL and UMEL and supports our assertion that terrestrial plant-based ^{14}C samples are most reliable in these lake sediments in a region where carbonate-bearing rocks are present. In 19-LMEL-U11, where paired terrestrial plant and bulk sediment-based radiocarbon ages were evaluated at 133.5 cm depth (Table 2), the bulk
270 sediment radiocarbon sample appeared to be ~800 years older than the terrestrial plant radiocarbon sample. Tentatively using this offset would place our local deglaciation timing before ~10,900 cal yr BP, which is within the uncertainty of the nearby estimates (Larsen et al., 2011; Carlson et al., 2014; Nelson et al., 2014). It should be noted that this offset is not constant over time, thus we do not use it to present a precise estimate of local deglaciation. Our results contribute to an overall consensus that local deglaciation occurred between 11,100-10,500 cal yr BP around Narsarsuaq (Larsen et al., 2011; Carlson et al., 2014;
275 Nelson et al., 2014). We strongly suspect that the demonstrated lake water ^{14}C reservoir effect at our sites explains the discrepancy in local deglaciation timing, but some of the offset may be due to small differences in elevation between the nearby 10Be sampling sites (~560 m a.s.l.), other lake site (~600 m a.s.l.) and our lake sites (~670 m a.s.l.).

5.3 The Neoglacial Narsarsuaq Advance: Timing and Ice Surface Elevation

280 Kiattuut Sermiat's Holocene terminal moraine sits ~8 km outboard of its historic (Little Ice Age) end moraine system. [10]Be ages from the terminal moraine indicates it was abandoned ~1500 cal yr BP (Winsor et al., 2014). It has been suggested based on culmination timing that the corresponding advance occurred just before 2000 cal yr BP (Bennike and Sparrenbom, 2007), but the exact timing of advance is unknown. Lake sediment records hold a unique ability to reconstruct the timing of ice advance into watersheds in addition to retreat. We argue that the sedimentological transition from organic lacustrine Unit 1c
285 to inorganic lacustrine Unit 1b in LMEL cores (Fig. 2) records a Neoglacial readvance of Kiattuut Sermiat, which dammed the lake system's outlet stream and created a proglacial lake that encompassed LMEL. This readvance was not captured by the UMEL cores, indicating that the ice elevation was between the elevations of the two lakes. This new evidence from lake sediments is consistent with geomorphic evidence for a Holocene glacial advance that dammed the valley, including the large lateral moraine and shoreline features (Figs. 1D and E). Readvance extensive enough to dam the valley occurred sometime
290 after 3900 cal yr BP based on a terrestrial plant based ^{14}C sample 1.5 cm below the transition in 19-LMEL-U11 (Fig. 4; Table 2). As discussed above, we believe terrestrial radiocarbon samples are the most reliable.

Kiattuut Sermiat remained at a quite stable advanced position, damming, and feeding sediments into LMEL but not UMEL, from ~3900-1600 cal yr BP. The sediment cores from LMEL and UMEL provide unusually precise constraints on the thickness of Kiattuut Sermiat during that Neoglacial advance. LMEL (elev. ~670 m a.s.l.) cores contain glaciolacustrine sediments

295 recording the advance, while UMEL (elev. ~675 m a.s.l.) cores do not (Figs. 2 and 3). As described earlier, there is extensive geomorphic evidence for Kiattuut Sermiat entering the E-W valley that contains the lakes and creating a glacially dammed ice-marginal lake. Upon retreat after ~1600 cal yr BP, it left behind a moraine/dam. This moraine/dam has a modern elevation of ~580 m a.s.l. which is lower than the modern elevation of LMEL (~670 m a.s.l.), suggesting the lake that encompassed LMEL was ice dammed. This ice-dammed lake would have filled the valley to the east of the moraine/dam roughly along the

300 670 m contour line on the modern landscape (Fig. 1C). The paleoshoreline features (Fig. 1E) indicate the lake reduced in size following the retreat of Kiattuut Sermiat and had its surface elevation set by the moraine at ~580 m a.s.l. This later version of the dammed lake did not contain modern LMEL or UMEL. This reveals that Kiattuut Sermiat had an ice surface elevation around ~670 m a.s.l. from ~3900-1600 cal yr BP at the location of the moraine/dam. This is ~250 m higher than the current ice elevation directly west of LMEL. Our elevation estimates do not account for glacial isostatic adjustment since subsequent

305 retreat; however, we suspect our estimate is within ~5 m of the true paleoglacier elevation. This is the difference in relative sea level change over the last 5000 years across south Greenland from Nanortalik to Qaqortoq (Sparrenbom et al., 2006; Sparrenbom et al., 2013).

Readvance of Kiattuut Sermiat after 3900 cal yr BP adds to evidence for widespread Neoglacial advance (~4500-3000 cal yr BP) of outlet glaciers, mountain glaciers, and ice caps across much of the southern half of Greenland (Larocca and Axford,

310 2022). The closest existing sedimentary glacial reconstruction recording an advance in the Middle to Late Holocene is from Lower Nordbosø (~15 km northwest of LMEL/UMEL; Fig. 5a; Larsen et al., 2011). It records the readvance of GrIS outlet glaciers at ~3000 cal yr BP. Quvnerit Lake ~160 km southeast of LMEL/UMEL records a mountain glacier readvance at ~3100 cal yr BP (Fig. 5a; Larocca et al., 2020a). Two smaller south Greenland mountain glacier systems studied by Larocca et al. (2020a) did not form until ~1300 cal yr BP, suggesting further cooling or wetter conditions at that time (Fig. 5a).

315
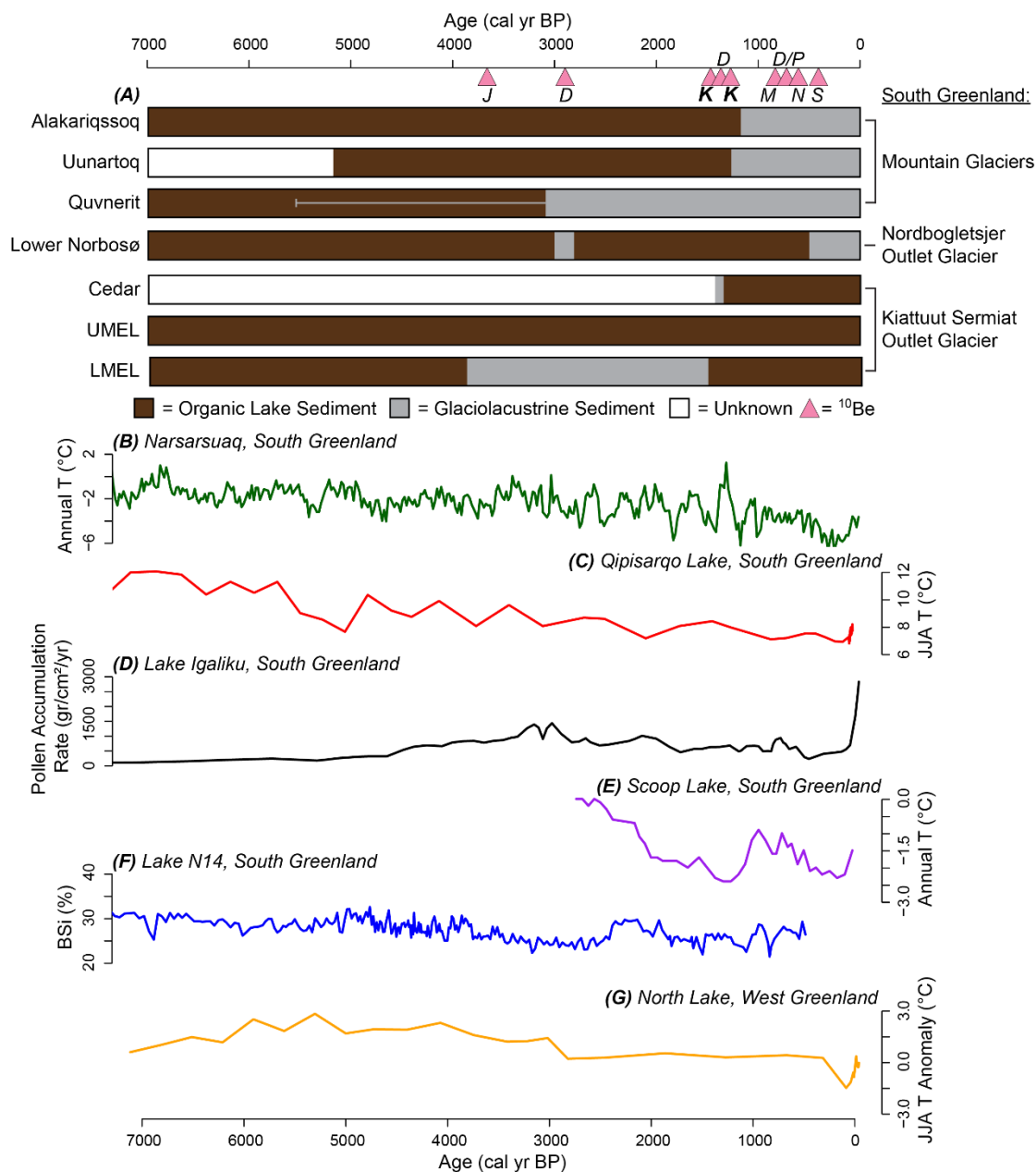
Figure 5 Summary of LMEL/UMEL sediment core changes and regional paleoclimate records for the Middle to Late Holocene. (A) Periods of glaciolacustrine (gray) vs. non-glaciolacustrine (brown) lake sediments in south Greenland sediment cores. Alakariqssoq, Uunartoq, and Quvnerit lakes reflect local mountain glaciers (Larocca et al., 2020a). Lower Nordbosø sediments reflect changes to Nordbogletsjer 15 km northwest of Kiattuut Sermiat (Larsen et al., 2011). Cedar Lake, LMEL, and UMEL sediments reflect Kiattuut Sermiat (Bennike and Sparrenbom, 2007; this study). Gray line (for Quvnerit) indicates times of reduced but detectable glacial input. Pink triangles indicate culmination timing from moraines in south Greenland.

J=Jespersen Bræ (Sinclair, 2019), D=DV2L (Biette et al., 2021), K=Kiattuut Sermiat (Nelson et al., 2014; Winsor et al., 2014), M=Mosquito glacier (informal name; Sinclair et al., 2019), P=Paarlit Sermiat (Sinclair et al., 2019), N=Naajat Sermiat (Sinclair et al., 2019), and S=Sermeq Kangilleq (Sinclair et al., 2019). (B) Annual temperature estimates for Narsarsuaq, South Greenland, based on Summit, Greenland, ice core $\delta^{15}N$ values combined with a climate model (Buizert et al., 2018). (C) Summer air temperatures inferred from pollen assemblages at Qipisarqo Lake (Fréchette and de Vernal, 2009). (D) Annual pollen grain accumulation rates at Lake Igaliku (Massa et al., 2012). (E) Chironomid head capsule oxygen isotope inferred annual air temperatures at Scoop Lake (Lasher and Axford, 2019). (F) Percent biogenic silica at Lake N14 (Andresen et al., 2004). (G) Chironomid assemblage-based summer air temperature anomalies relative to present at North Lake in western Greenland (Axford et al., 2013).

[10]Be ages from the outermost Holocene moraine deposited by Jespersen Bræ, which drains the Julianehåb Ice Cap (~25 km east/southeast of LMEL/UMEL), indicates a Late Holocene culmination at ~3700 cal yr BP (Fig. 5a; Sinclair, 2019). An additional set of [10]Be samples from the outermost moraines deposited by the DV2L mountain glacier (~50 km southeast of LMEL/UMEL) indicates a culmination age of ~2900 cal yr BP (Fig. 5a; Biette et al., 2021). These culmination ages imply Middle to Late Holocene glacier advances followed by retreat at these times. Many other outermost moraines record younger Late Holocene culmination ages in south Greenland (Sinclair, 2019; Biette et al., 2021), but this could be due to later glacial advances destroying moraines deposited in prior Neoglacial advances. The majority of records that can address the Neoglacial advance in south Greenland indicate it occurred between ~4000-3000 cal yr BP.

Farther afield in southeast Greenland, Kulusuk Lake indicates a mountain glacier advanced at 4100, 3900, and 3200 cal yr BP (~630 km northeast of LMEL/UMEL; Balascio et al., 2015). 60 km north of Kulusuk Lake, [10]Be ages from outermost moraines deposited by the TAS-A and TAS-B mountain glaciers have culmination ages at ~3300 and ~3750 cal yr BP, respectively (Biette et al., 2021). This evidence suggests a similar timing for Neoglacial advance in southeast Greenland (~4000-3000 cal yr BP).

In southwest Greenland, Lake 09370 records an advance of a GrIS outlet glacier at ~3700 cal yr BP (~290 km northwest of LMEL/UMEL; Larsen et al., 2015). Four other southwest Greenland lakes that received glacial meltwater from GrIS outlet glaciers at some point in their past did not record a Neoglacial advance (Larsen et al., 2015). Langesø Lake and Badesø Lake of southwest Greenland record advances of local mountain glaciers into their catchments at ~3600 and ~3500 cal yr BP, respectively (~450 km northwest of LMEL/UMEL; Larsen et al., 2017). The third reconstruction presented by Larsen et al. (2017) from Lake IS21 did not record a Neoglacial advance of a local ice cap. Crash Lake of southwest Greenland records an overall trend of advancing Sukkertoppen glaciers and ice caps after ~4600 cal yr BP with centennial scale variations (Schweinsberg et al., 2018). Pers Lake of southwest Greenland records small glacial meltwater inputs beginning at ~4300 cal yr BP indicating the growth of nearby mountain glaciers (Larocca et al., 2020b). Overall, evidence from this region appears more mixed, with several outlet glacier reconstructions showing no signs of a Neoglacial advance. This could be explained by the greater climate sensitivity of mountain glaciers compared to outlet glaciers and ice caps and/or the glacial advances not

reaching the watersheds of the sampled threshold lakes. Regardless, it appears that the Neoglacial readvance was registered slightly earlier in southwest Greenland, from ~4500-3500 cal yr BP. Finally, in west Greenland, Sikuiui Lake captured ice cap growth at 5000 cal yr BP, with further glacial expansion at ~3700 cal yr BP (~1040 km north/northwest of LMEL/UMEL;

360 Schweinsberg et al., 2017).

Paleoclimate records from south Greenland support that glacial advances were driven by regional cooling between ~4500-3000 cal yr BP. Pollen assemblages from Qipisarqo Lake (~130 km west of LMEL/UMEL) suggest July surface air temperatures cooled at a rate of 0.5°C per 1,000 years over the last ~7,000 years (Fig. 5c; Fréchette and de Vernal, 2009). Another temperature record from Qipisarqo Lake based on chironomid head capsule oxygen isotope values finds similar

365 results, with mean annual temperatures decreasing ~4°C from 8300 cal yr BP to present (Wooller et al., 2004). A third record from Qipisarqo Lake suggests the onset of Neoglacial cooling occurred at ~3000 cal yr BP based on decreasing biogenic silica and organic content of the sediment (Kaplan et al., 2002). Pollen assemblages from Lake Igaliku (~30 km south of LMEL/UMEL) indicate that moister and cooler conditions began at ~4700 cal yr BP and pollen assemblages and accumulation rates suggest cooling was enhanced after 3000 cal yr BP (Fig. 5d; Massa et al., 2012). At Scoop Lake (~60 km south of

370 LMEL/UMEL), Neoglacial cooling of ~2°C occurred from ~3000-1500 cal yr BP based on a chironomid oxygen isotope reconstruction (Fig. 5e; Lasher and Axford, 2019). A reconstruction of biogenic silica and minerogenic content of sediment from Lake N14 at the southern tip of Greenland indicates that cooling likely began at ~4700 cal yr BP with enhanced cooling after ~3700 cal yr BP (Fig. 5f; Andresen et al., 2004). Farther away, near Ilulissat in west Greenland (~920 km northwest of LMEL/UMEL), a chironomid assemblage-based temperature reconstruction from North Lake reconstructs a summer cooling

375 of 2-3°C from ~4000-200 cal yr BP (Fig. 5g; Axford et al., 2013).

Marine records near south Greenland also indicate Neoglacial cooling and/or glacial advance. A marine sediment core (PO 243-451) from the Igaliku Fjord of south Greenland indicates cool and stratified water-column conditions at ~3200-2800 cal yr BP and ~2600-2300 cal yr BP based on foraminifera species (Lassen et al., 2004). Another marine sediment record from the Narsaq Sound of south Greenland suggests Neoglaciation began at ~4800 cal yr BP due to ice rafted debris peaks at 4600

380 and 3600 cal yr BP (Nørgaard-Pedersen and Mikkelsen, 2009). A marine core from the Ameralik Fjord of southwest Greenland indicates the onset of Neoglaciation at ~3200 cal yr BP based on foraminifera species (Seidenkrantz et al., 2007). Just off the coast of southeast Greenland, a multiproxy record developed on core JM96-1206/2GC suggests the East Greenland Current, which carries cold Arctic water to south Greenland, strengthened and forced the relatively warm, Atlantic-sourced Irminger Current water to the subsurface during the Neoglacial beginning at ~4500 cal yr BP (Perner et al., 2016).

385 In summary, data indicate that a cooling-driven advance of many GrIS outlet glaciers, mountain glaciers, and ice caps in the southern sectors of Greenland occurred between ~4500-3000 cal yr BP and our record adds to that evidence. The main drivers of overall cooling through the Middle to Late Holocene in south Greenland were decreasing Northern Hemisphere summer insolation (Berger and Loutre, 1999) and increased delivery of cold, Arctic waters via the strengthening East Greenland Current (Perner et al., 2016).

390

5.4 Late Holocene Retreat from the Narsarsuaq Moraine

All LMEL sediment cores record a transition from minerogenic, glaciolacustrine sediment (Unit 1b) to organic lake sediments (Unit 1a) which represents a local retreat of Kiattuut Sermiat in the Late Holocene (Fig. 2a). One mixed terrestrial and aquatic plant radiocarbon sample 2.5 cm above the transition indicates that the Kiattuut Sermiat surface elevation decrease occurred near or just prior to ~1600 cal yr BP, and related ages from aquatic plants or bulk sediments support this age though they presumably reflect large reservoir effects (Fig. 4; Table 2). We cannot definitively say that retreat occurred before ~1600 cal yr BP, as aquatic organic materials at LMEL are subject to a reservoir effect and likely reflect ages that are too old.

Nonetheless, this age constraint is consistent with reconstructions from the terminus of Kiattuut Sermiat that indicate the outlet glacier retreated between ~1600-1300 cal yr BP. At Cedar Lake, which is ~13 km southwest of LMEL/UMEL and within the outermost moraines deposited by Kiattuut Sermiat, terrestrial plant-based radiocarbon samples from just above the minerogenic to organic lake sediment transition indicate Kiattuut Sermiat retreated prior to ~1300 cal yr BP (Fig. 5a; Bennike and Sparrenbom, 2007). Winsor et al. (2014) reported several [10]Be samples from the outermost moraines deposited by Kiattuut Sermiat with a mean age of ~1500 cal yr BP, indicating the culmination timing of the largest advance of this outlet glacier (Fig. 5a). Another [10]Be sample from a boulder downstream of Kiattuut Sermiat also indicated culmination at ~1500 cal yr BP (Nelson et al., 2014).

Retreat of Kiattuut Sermiat at ~1500 cal yr BP contrasts conspicuously with the strong evidence for regional cooling at this time, and with the majority of published glacier reconstructions from the region. Nearby, Lower Nordbosø sediment indicates a GrIS outlet glacier retreated from its catchment at ~2800 cal yr BP and remained out of the catchment until 500 cal yr BP (Fig. 5a; Larsen et al., 2011). Quvnerit Lake, Alakariqssoq Lake, and Uunartoq Lake of south Greenland record the constant presence of mountain glaciers in their watersheds from 3100 cal yr BP to present, 1300 cal yr BP to present, and 1200 cal yr BP to present, respectively (Fig. 5a; Larocca al., 2020a). An outermost moraine deposited by Naajat Sermiat (GrIS outlet glacier; ~75 km west/southwest of LMEL/UMEL) of south Greenland has been dated to ~600 cal yr BP (Fig. 5a; Sinclair, 2019). A south Greenland moraine formed by Sermeq Kangilleq (Julianehåb Ice Cap outlet glacier; 40 km southeast of LMEL/UMEL) has been [10]Be sampled and dated to ~400 cal yr BP (Fig. 5a; Sinclair, 2019). Paarlit Sermiat, an outlet glacier draining an unnamed ice cap ~125 km southeast of LMEL/UMEL, deposited a moraine at ~700 cal yr BP based on [10]Be ages (Fig. 5a; Sinclair, 2019). A mountain glacier (Mosquito Glacier; ~110 km southeast of LMEL/UMEL) moraine stabilized at ~800 cal yr BP (Fig. 5a; Sinclair, 2019). One moraine was deposited by the DV2L mountain glacier of south Greenland at ~1400 cal yr BP based on [10]Be samples (Biette et al., 2021). This final moraine [10]Be age is the only other evidence from south Greenland indicating a culmination and retreat timing of an outermost moraine around ~1500 cal yr BP.

In southeast Greenland, only one [10]Be dated moraine shows a similar culmination timing to Kiattuut Sermiat at around 1500 cal yr BP (Biette et al., 2021). The remaining lake sediment (Balascio et al., 2015) and moraine (Biette et al., 2021) based glacial reconstructions from this region show no sign of retreat at this time. A larger number of lake sediment based glacial reconstructions exist in southwest Greenland and show mixed evidence. Three lake records show outlet glacier and ice cap retreat within a few hundred years of Kiattuut Sermiat's retreat including 09370 Lake (Larsen et al., 2015), Frederikshåb

Isblink (Larsen et al., 2015), and Lake IS21 (Larsen et al., 2017). However, each of these records also shows an advance of equal or larger magnitude occurring in the past millennium, unlike Kiattuut Sermiat. Several other records show no sign of retreat around 1500 cal yr BP, including Kan01 Lake (Larsen et al., 2015), Langesø Lake (Larsen et al., 2017), Badesø Lake (Larsen et al., 2017), Crash Lake (Schweinsberg et al., 2018), and Pers Lake (Larocca et al., 2020a).

Climate records from the southern half of Greenland show an overall cooling trend through the Middle to Late Holocene with some showing a brief period of warming during the Medieval Climate Anomaly before cooling again during the Little Ice Age (Fig. 5B-G; Kaplan et al., 2002; Andresen et al., 2004; Wooller et al., 2004; Fréchette and de Vernal, 2009; Massa et al., 2012; Axford et al., 2013; Buizert et al., 2018; Lasher and Axford, 2019). Nearby marine records corroborate a cooling trend in the Late Holocene with warming during the Medieval Climate Anomaly followed by cooling during the Little Ice Age (Lassen et al., 2004; Seidenkrantz et al., 2007; Nørgaard-Pedersen and Mikkelsen, 2009). This Late Holocene cooling drove glacial advances across Greenland, presumably including Kiattuut Sermiat. However, warming during the Medieval Climate Anomaly appears too late to be the driver of Kiattuut Sermiat's Late Holocene retreat. Rather than temperature, the retreat of Kiattuut Sermiat at ~1500 cal yr BP could potentially be driven by differing precipitation amounts. Late Holocene precipitation amount reconstructions from Greenland are limited to relatively high elevation ice core sites and reflect variable conditions (Cuffey and Clow, 1997; Badgeley et al., 2020; Osman et al., 2021). Because of this, it is unclear if a local precipitation reduction could have potentially driven Kiattuut Sermiat retreat. Another potential factor is that Kiattuut Sermiat is located where the GrIS meets the Julianehåb Ice Cap and where passive ice margins meet fast-flowing outlet glaciers (Larsen et al., 2011). This local glaciological complexity in combination with any local precipitation reduction could potentially account for the unusual timing and magnitude of Kiattuut Sermiat's Late Holocene retreat.

Another unusual, although not unique, feature of Kiattuut Sermiat's history is that its advance during the Little Ice Age was notably lesser than the earlier Neoglacial Narsarsuaq advance. We find that Kiattuut Sermiat did not readvance into the LMEL or UMEL watersheds during the Little Ice Age, consistent with the location of the glacier's Little Ice Age moraines just outside of the modern glacier terminus and within its Narsarsuaq advance terminus (Winsor et al., 2015). This is unlike the response of most studied glaciers in Greenland which deposited their outermost Late Holocene moraines during the Little Ice Age (Kelly and Lowell, 2009; Kjær et al., 2022). Little Ice Age glacier maxima are consistent with widespread evidence that progressive insolation-driven cooling made the last millennium the coldest period of the Middle to Late Holocene across much of Greenland and the Arctic (Kaufman et al., 2009; Briner et al., 2016). During the Little Ice Age, GISP2, DYE3, and Nuussuaq ice cores all suggest lower precipitation amounts than present (Cuffey and Clow, 1997; Badgeley et al., 2020; Osman et al., 2021) which could indicate Kiattuut Sermiat is highly sensitive to changes in precipitation given its limited advance compared to other nearby south Greenland outlet glaciers (Larsen et al., 2011).

6 Conclusions

Sedimentary records from two adjacent upland lakes substantially improve our understanding of the Late Holocene history of a GrIS outlet glacier. We reconstruct the timing and thickness of the major Neoglacial advance of Kiattuut Sermiat and confirm

the timing of its subsequent Late Holocene retreat. Our ^{14}C-based age constraint on regional deglaciation timing (~11,700 cal yr BP) is slightly older than the timing from [10]Be samples around Narsarsuaq (~11,000 cal yr BP), likely due to a reservoir effect in aquatic plant radiocarbon samples. We find that the Neoglacial advance of Kiattuut Sermiat that deposited the Narsarsuaq end moraines dammed a tributary ice-marginal upland valley, creating an ice-dammed lake. The temporary ice-dammed lake subsumed one of our study lakes, LMEL, after ~3900 cal yr BP. The slightly higher-elevation adjacent lake, UMEL, remained outside the limits of the ice-dammed lake, indicating an ice dam elevation of ~670 m. This advance was presumably driven by regional cooling that led to the advance of many Greenland glaciers between ~4500-3000 cal yr BP. The Kiattuut Sermiat ice surface and the lake it dammed were maintained at ~670 m until ~1600 cal yr BP, when LMEL sediments show a transition back to organic, non-glacier influenced lake sediments for the remainder of the record. Ice lowering and the associated frontal retreat documented in previous work occurred during an apparent period of regional cooling and may have been caused by changes in precipitation amounts and/or related to the glaciological complexity of this outlet glacier, which is influenced by the Julianehåb Ice Cap adjacent to the GrIS. In the future, high-resolution ice sheet models could be used to further determine what factors drove Kiattuut Sermiat retreat at this time, and what explained the relatively small magnitude of this outlet glacier's Little Ice Age advance compared with the extensive Late Holocene Narsarsuaq advance.

Data Availability

The LMEL and UMEL radiocarbon, magnetic susceptibility, and titanium concentration data are available at the National Centers for Environmental Information/the NOAA paleoclimate data archive: https://www.ncei.noaa.gov/access/paleo-search/study/37700.

Supplement

The supplement related to this article is available online at:

Author Contributions

PP contributed to funding acquisition, field work, laboratory work, formal analysis, visualization, data curation, writing of the draft manuscript, review of the draft manuscript. YA contributed to conceptualization, funding acquisition, project administration, resources, supervision, writing of the draft manuscript, and review of the draft manuscript.

Competing Interests

The authors declare that they have no conflict of interest.

Acknowledgements

We thank Grace Schellinger, Mia Tuccillo, Bailey Nash, Aidan Burdick, and Sophia Liu for assistance with lab work. Additional thanks go to Laura Larocca, G. Everett Lasher, Tim Coston, Aaron Hartz, Kyli Cosper and Polar Field Services,

the U.S. Air National Guard, Jacky Simoud and Blue Ice Explorer, and Air Greenland for assistance during field work. We also thank Sarah Woodroffe for helpful discussions regarding isostasy. We are appreciative of the Woods Hole Oceanographic Institution - National Ocean Sciences Accelerator Mass Spectrometry facility and Beta Analytic for radiocarbon analysis. We are grateful to the people and Government of Greenland for allowing us to work on their land. Samples were collected with permission of the Government of Greenland's (Naalakkersuisut) scientific survey license VU-00160 and minerals export permit 025/2019. DEMs were provided by the Polar Geospatial Center under NSF-OPP awards 1043681, 1559691, and 1542736.

Financial Support

This work was supported financially by NSF OPP awards 1454734 and 2002515 to Yarrow Axford and an NSF Graduate Research Fellowship to Peter Puleo.

References

Adamson, K., Lane, T., Carney, M., Delaney, C., Howden, A.: The imprint of catchment processes on Greenlandic ice cap proglacial lake records: analytical approaches and palaeoenvironmental significance. Journal of Quaternary Science 37, 1388-1406, 2022.

Andresen, C.S., Björck, S., Bennike, O., Bond, G.: Holocene climate changes in southern Greenland: evidence from lake sediments. Journal of Quaternary Science 19, 783-795, 2004.

Axford, Y., De Vernal, A., Osterberg, E.C.: Past Warmth and Its Impacts During the Holocene Thermal Maximum in Greenland. Annual Review of Earth and Planetary Sciences 49, 279-307, 2021.

Axford, Y., Losee, S., Briner, J.P., Francis, D.R., Langdon, P.G., Walker, I.R.: Holocene temperature history at the western Greenland Ice Sheet margin reconstructed from lake sediments. Quaternary Science Reviews 59, 87-100, 2013.

Badgeley, J.A., Steig, E.J., Hakim, G.J., Fudge, T.J.: Greenland temperature and precipitation over the last 20 000 years using data assimilation. Climate of the Past 16, 1325-1346, 2020.

Balascio, N.L., amp, apos, Andrea, W.J., Bradley, R.S.: Glacier response to North Atlantic climate variability during the Holocene. Climate of the Past 11, 1587-1598, 2015.

Bennike, O., Sparrenbom, C.J.: Dating of the Narssarssuaq stade in southern Greenland. The Holocene 17, 279-282, 2007.

Berger, A., Loutre, M.F.: Insolation Values for the Climate of the Last 10 Million Years. Quaternary Science Reviews 10, 297-317, 1999.

Biette, M., Jomelli, V., Chenet, M., Braucher, R., Menviel, L., Swingedouw, D., Rinterknecht, V.: Evidence of the largest Late Holocene mountain glacier extent in southern and southeastern Greenland during the middle Neoglacial from [10]Be moraine dating. Boreas, 1-17, 2021.

Bjørk, A.A., Kruse, L.M., Michaelsen, P.B.: Brief communication: Getting Greenland's glaciers right – a new data set of all official Greenlandic glacier names. The Cryosphere 9, 2215-2218, 2015.

Björck, S., Bennike, O., Rosén, P., Andresen, C.S., Bohncke, S., Kaas, E., Conley, D.J.: Anomalously mild Younger Dryas summer conditions in southern Greenland. Geology 30, 427-430, 2002.

Björck, S., Wohlfarth, B.: [14]C Chronostratigraphic Techniques in Paleolimnology in: Last, W.M., Smol, J.P. (Eds.), Tracking Environmental Change Using Lake Sediments. Volume 1: Basin Analysis, Coring, and Chronological Techniques. Kluwer Academic Publishers, Dordrecht, 205-245, 2001.

Briner, J.P., McKay, N.P., Axford, Y., Bennike, O., Bradley, R.S., de Vernal, A., Fisher, D., Francus, P., Fréchette, B., Gajewski, K., Jennings, A., Kaufman, D.S., Miller, G., Rouston, C., Wagner, B.: Holocene climate change in Arctic Canada and Greenland. Quaternary Science Reviews 147, 340-364, 2016.

Buizert, C., Keisling, B.A., Box, J.E., He, F., Carlson, A.E., Sinclair, G., DeConto, R.M.: Greenland-Wide Seasonal Temperatures During the Last Deglaciation. Geophysical Research Letters 45, 1905-1914, 2018.

Cappelen, J.: Climatological Standard Normals 1981-2010 - Denmark, The Faroe Islands and Greenland - Based on Data Published in DMI Reports 18-02, 18-04 and 18-05. DMI Report 18-19, DMI, Copenhagen, 2019.

Carlson, A.E., Winsor, K., Ullman, D.J., Brook, E.J., Rood, D.H., Axford, Y., LeGrande, A.N., Anslow, F.S., Sinclair, G.: Earliest Holocene south Greenland ice sheet retreat within its late Holocene extent. Geophysical Research Letters 41, 5514-5521, 2014.

Cuffey, K.M., Clow, G.D.: Temperature, accumulation, and ice sheet elevation in central Greenland through the last deglacial transition. Journal of Geophysical Research: Oceans 102, 26383-26396, 1997.

Dowdeswell, J.A.: Atmospheric science. The Greenland Ice Sheet and global sea-level rise. Science 311, 963-964, 2006.

Fréchette, B., De Vernal, A.: Relationship between Holocene climate variations over southern Greenland and eastern Baffin Island and synoptic circulation pattern. Climate Past 5, 347-359, 2009.

Goelzer, H., Nowicki, S., Payne, A., Larour, E., Seroussi, H., Lipscomb, W.H., Gregory, J., Abe-Ouchi, A., Shepherd, A., Simon, E., Agosta, C., Alexander, P., Aschwanden, A., Barthel, A., Calov, R., Chambers, C., Choi, Y., Cuzzone, J., Dumas, C., Edwards, T., Felikson, D., Fettweis, X., Golledge, N.R., Greve, R., Humbert, A., Huybrechts, P., Le clec'h, S., Lee, V., Leguy, G., Little, C., Lowry, D.P., Morlighem, M., Nias, I., Quiquet, A., Rückamp, M., Schlegel, N.-J., Slater, D.A., Smith, R.S., Straneo, F., Tarasov, L., van de Wal, R., van den Broeke, M.: The future sea-level contribution of the Greenland ice sheet: a multi-model ensemble study of ISMIP6. The Cryosphere 14, 3071-3096, 2020.

Greve, R., Chambers, C.: Mass loss of the Greenland ice sheet until the year 3000 under a sustained late-21st-century climate. Journal of Glaciology 68, 618-624, 2022.

Kaplan, M.R., Wolfe, A.P., Miller, G.H.: Holocene Environmental Variability in Southern Greenland Inferred from Lake Sediments. Quaternary Research 58, 149-159, 2002.

Karlen, W., Matthews, J.A.: Reconstructing Holocene Glacier Variations from Glacial Lake Sediments: Studies from Nordvestlandet and Jostedalsbreen-Jotunheimen, Southern Norway. Geogr Ann A 74, 327-348, 1992.

Kaufman, D.S., Schneider, D.P., McKay, N.P., Ammann, C.M., Bradley, R.S., Briffa, K.R., Miller, G.H., Otto-Bliesner, B.L., Overpeck, J.T., Vinther, B.M., Arctic Lakes 2k Project Members: Recent warming reverses long-term arctic cooling. Science 325, 1236-1239, 2009.

Kelly, M.A., Lowell, T.V.: Fluctuations of local glaciers in Greenland during latest Pleistocene and Holocene time. Quaternary Science Reviews 28, 2088-2106, 2009.

Kjær, K.H., Bjørk, A.A., Kjeldsen, K.K., Hansen, E.S., Andresen, C.S., Siggaard-Andersen, M.-L., Khan, S.A., Søndergaard, A.S., Colgan, W., Schomacker, A., Woodroffe, S., Funder, S., Rouillard, A., Jensen, J.F., Larsen, N.K.: Glacier response to the Little Ice Age during the Neoglacial cooling in Greenland. Earth-Science Reviews 227, 1-43, 2022.

Larocca, L.J., Axford, Y.: Arctic glaciers and ice caps through the Holocene:a circumpolar synthesis of lake-based reconstructions. Climate of the Past 18, 579-606, 2022.

Larocca, L.J., Axford, Y., Bjørk, A.A., Lasher, G.E., Brooks, J.P.: Local glaciers record delayed peak Holocene warmth in south Greenland. Quaternary Science Reviews 241, 106421, 1-16, 2020a.

Larocca, L.J., Axford, Y., Woodroffe, S.A., Lasher, G.E., Gawin, B.: Holocene glacier and ice cap fluctuations in southwest Greenland inferred from two lake records. Quaternary Science Reviews 246, 2020b.

Larsen, N.K., Kjær, K.H., Lecavalier, B., Bjørk, A.A., Colding, S., Huybrechts, P., Jakobsen, K.E., Kjeldsen, K.K., Knudsen, K.-L., Odgaard, B.V., Olsen, J.: The response of the southern Greenland ice sheet to the Holocene thermal maximum. Geology 43, 291-294, 2015.

Larsen, N.K., Kjær, K.H., Olsen, J., Funder, S., Kjeldsen, K.K., Nørgaard-Pedersen, N.: Restricted impact of Holocene climate variations on the southern Greenland Ice Sheet. Quaternary Science Reviews 30, 3171-3180, 2011.

Larsen, N.K., Strunk, A., Levy, L.B., Olsen, J., Bjørk, A., Lauridsen, T.L., Jeppesen, E., Davidson, T.A.: Strong altitudinal control on the response of local glaciers to Holocene climate change in southwest Greenland. Quaternary Science Reviews 168, 69-78, 2017.

Lasher, G.E., Axford, Y.: Medieval warmth confirmed at the Norse Eastern Settlement in Greenland. Geology 47, 267-270, 2019.

Lassen, S.J., Kuijpers, A., Kunzendorf, H., Hoffmann-Wieck, G., Mikkelsen, N., Konradi, P.: Late-Holocene Atlantic bottom-water variability in Igaliku Fjord, South Greenland, reconstructed from foraminifera faunas. The Holocene 14, 165-171, 2004.

Levy, L.B., Larsen, N.K., Knudsen, M.F., Egholm, D.L., Bjørk, A.A., Kjeldsen, K.K., Kelly, M.A., Howley, J.A., Olsen, J., Tikhomirov, D., Zimmerman, S.R.H., Kjær, K.H.: Multi-phased deglaciation of south and southeast Greenland controlled by climate and topographic setting. Quaternary Science Reviews 242, 1-12, 2020.

Massa, C., Perren, B.B., Gauthier, É., Bichet, V., Petit, C., Richard, H.: A multiproxy evaluation of Holocene environmental change from Lake Igaliku, South Greenland. Journal of Paleolimnology 48, 241-258, 2012.

Monnin, E., Indermuhle, A., Dallenbach, A., Fluckiger, J., Stauffer, B., Stocker, T.F., Raynaud, D., Barnola, J.M.: Atmospheric CO_2 concentrations over the last glacial termination. Science 291, 112-114, 2001.

Nelson, A.H., Bierman, P.R., Shakun, J.D., Rood, D.H.: Using in situ cosmogenic [10]Be to identify the source of sediment leaving Greenland. Earth Surface Processes and Landforms 39, 1087-1100, 2014.

Nesje, A.: A Piston Corer for Lacustrine and Marine-Sediments. Arctic and Alpine Research 24, 257-259, 1992.

Nørgaard-Pedersen, N., Mikkelsen, N.: 8000 year marine record of climate variability and fjord dynamics from Southern Greenland. Marine Geology 264, 177-189, 2009.

Oerlemans, J.: Glaciers and Climate Change. Balkema, Lisse, 2001.

Osman, M.B., Smith, B.E., Trusel, L.D., Das, S.B., McConnell, J.R., Chellman, N., Arienzo, M., Sodemann, H.: Abrupt
600 Common Era hydroclimate shifts drive west Greenland ice cap change. Nature Geoscience 14, 756-761, 2021.

Perner, K., Jennings, A.E., Moros, M., Andrews, J.T., Wacker, L.: Interaction between warm Atlantic-sourced waters and the
East Greenland Current in northern Denmark Strait (68°N) during the last 10 600 cal a BP. Journal of Quaternary Science 31,
472-483, 2016.

Porter, C., Morin, P., Howat, I., Noh, M.J., Bates, B., Peterman, K., Keesey, S., Schlenk, M., Gardiner, J., Tomko, K., Willis,
605 M., Kelleher, C., Cloutier, M., Husby, E., Foga, S., Nakamura, H., Platson, M., Wethington, M., Williamson, C., Bauer, G.,
Enos, J., Arnold, G., Kramer, W., Becker, P., Doshi, A., D'Souza, C., Cummens, P., Laurier, F., Bojesen, M.: ArcticDEM,
Harvard Dataverse V1, https://doi.org/10.7910/DVN/OHHUKH, 2018.

Puleo, P.J.K., Masterson, A.L., Medeiros, A.S., Schellinger, G., Steigleder, R., Woodroffe, S., Osburn, M.R., Axford, Y.:
Younger Dryas and early Holocene climate in south Greenland inferred from oxygen isotopes of chironomids, aquatic Moss,
610 and Moss cellulose. Quaternary Science Reviews 296, 1-16, 2022.

Reimer, P.J., Austin, W.E.N., Bard, E., Bayliss, A., Blackwell, P.G., Bronk Ramsey, C., Butzin, M., Cheng, H., Edwards, R.L.,
Friedrich, M., Grootes, P.M., Guilderson, T.P., Hajdas, I., Heaton, T.J., Hogg, A.G., Hughen, K.A., Kromer, B., Manning,
S.W., Muscheler, R., Palmer, J.G., Pearson, C., van der Plicht, J., Reimer, R.W., Richards, D.A., Scott, E.M., Southon, J.R.,
Turney, C.S.M., Wacker, L., Adolphi, F., Büntgen, U., Capano, M., Fahrni, S.M., Fogtmann-Schulz, A., Friedrich, R., Köhler,
615 P., Kudsk, S., Miyake, F., Olsen, J., Reinig, F., Sakamoto, M., Sookdeo, A., Talamo, S.: The IntCal20 Northern Hemisphere
Radiocarbon Age Calibration Curve (0–55 cal kBP). Radiocarbon 62, 725-757, 2020.

Schweinsberg, A.D., Briner, J.P., Miller, G.H., Bennike, O., Thomas, E.K.: Local glaciation in West Greenland linked to North
Atlantic Ocean circulation during the Holocene. Geology 45, 195-198, 2017.

Schweinsberg, A.D., Briner, J.P., Miller, G.H., Lifton, N.A., Bennike, O., Graham, B.L.: Holocene mountain glacier history
620 in the Sukkertoppen Iskappe area, southwest Greenland. Quaternary Science Reviews 197, 142-161, 2018.

Seidenkrantz, M.S., Aagaard-Sørensen, S., Sulsbrück, H., Kuijpers, A., Jensen, K.G., Kunzendorf, H.: Hydrography and
climate of the last 4400 years in a SW Greenland fjord: implications for Labrador Sea palaeoceanography. The Holocene 17,
387-401, 2007.

625 Sinclair, G.: North Atlantic Climate and Cryosphere Variability Over the Past 20,000 Years, College of Earth, Ocean, and Atmospheric Sciences. Oregon State University, 1-248, 2019.

Sparrenbom, C., Bennike, O., Björck, S., Lambeck, K.: Holocene relative sea-level changes in the Qaqortoq area, southern Greenland. Boreas 35, 171-187, 2006.

Sparrenbom, C.J., Bennike, O., Fredh, D., Randsalu-Wendrup, L., Zwartz, D., Ljung, K., Björck, S., Lambeck, K.: Holocene relative sea-level changes in the inner Bredefjord area, southern Greenland. Quaternary Science Reviews 69, 107-124, 2013.

630 Steenfelt, A., Kolb, J., Thrane, K.: Metallogeny of South Greenland: A review of geological evolution, mineral occurrences and geochemical exploration data. Ore Geology Reviews 77, 194-245, 2016.

Stuiver, M., Reimer, P.J., and Reimer, R.W.: CALIB 8.2, http://calib.org, accessed 9/22/2022, 2022.

Upton, B., Emeleus, C.H., Heaman, L.M., Goodenough, K.M., Finch, A.A.: Magmatism of the mid-Proterozoic Gardar Province, South Greenland: chronology, petrogenesis and geological setting. Lithos 68, 43-65, 2003.

635 Weidick, A.: Ice Margin Features in the Julianehåb District, south Greenland. Reitzel, 1963.

Winsor, K., Carlson, A.E., Rood, D.H.: [10]Be dating of the Narsarsuaq moraine in southernmost Greenland: evidence for a late-Holocene ice advance exceeding the Little Ice Age maximum. Quaternary Science Reviews 98, 135-143, 2014.

Wooller, M.J., Francis, D., Fogel, M.L., Miller, G.H., Walker, I.R., Wolfe, A.P.: Quantitative paleotemperature estimates from d18O of chironomid head capsules preserved in arctic lake sediments. Journal of Paleolimnology 31, 267-274, 2004.

640